Coherent transition radiation in the far-infrared region

Yukio Shibata, Kimihiro Ishi, Toshiharu Takahashi, Toshinobu Kanai, Fumitaka Arai, Shin-ichi Kimura, Toshiaki Ohsaka, and Mikihiko Ikezawa
Research Institute for Scientific Measurements, Tohoku University, Katahira, Sendai 980, Japan

Yasuhiro Kondo
Faculty of Engineering, Tohoku University, Aramaki, Sendai 980, Japan

Ryukou Kato, Shigekazu Urasawa, Toshiharu Nakazato, Satoshi Niwano, Masahiro Yoshioka, and Masayuki Oyamada
Laboratory of Nuclear Science, Tohoku University, Mikamine, Sendai 982, Japan
(Received 6 July 1993)

Coherent transition radiation (TR) has been observed in the wavelength range from 0.2 to 5 mm, which is emitted from bunches of 150-MeV electrons passing through a radiator system composed of an upstream aluminum foil and a downstream aluminum mirror. At the beam current of 1 μA, the intensity at $\lambda=1$ mm is enhanced by a factor of 0.9×10^6 compared with incoherent TR. The value of this factor is close to the number of electrons in the bunch. The intensity of the TR has been observed to depend on the emission length or the length of the trajectory of the electrons between the foil and the mirror. The angular distribution of the TR intensity and its dependence on the wavelength and on the emission length have been observed. All results are in good agreement with theory. Dependences of the TR intensity on the cross section of the beam and on the radiation material have also been examined. From the observed spectrum of TR, the longitudinal distribution function of electrons in the bunch is derived to be approximately a Gaussian with the bunch length full width at half maximum of 0.28 mm.

PACS number(s): 41.75.Fr, 42.72.Ai, 41.60.Ap

I. INTRODUCTION

Transition radiation (TR) is emitted when an electron crosses a boundary of two media [1–3]. At short wavelengths from the x-ray region to the visible region, TR has been studied theoretically and experimentally over several decades. In the infrared region, however, there had been no investigation of TR because of its weak intensity. Recently, experiments of coherent TR using a short-bunch electron beam were carried out, and it has been found that TR is enormously enhanced due to the coherence effect in the far-infrared region where the wavelength is comparable to or longer than the longitudinal bunch length [4–6]. The coherence effect of TR is analogous to that of coherent synchrotron radiation [7–11].

According to the theory [3,12], TR is not emitted instantaneously at the boundary, but occurs over a formation length. When an electron crosses a metallic foil in vacuum, the intensity P_e of forward TR is given as follows, provided that a distance between the boundary and an observation point is much longer than the formation length:

$$P_e=\frac{\alpha\beta^2\sin^2\theta\cos^2\theta}{\pi^2\lambda(1-\beta^2\cos^2\theta)^2}|\zeta|^2 d\Omega\, d\lambda\ , \tag{1}$$

$$\zeta=\frac{(\epsilon-1)[1-\beta^2-\beta(\epsilon-\sin^2\theta)^{1/2}]}{[\epsilon\cos\theta+(\epsilon-\sin^2\theta)^{1/2}][1-\beta(\epsilon-\sin^2\theta)^{1/2}]}\ , \tag{2}$$

where α is the fine-structure constant, β the ratio of the speed of the electron to that of light in vacuum, θ the direction angle from the axis of the electron beam, ϵ the dielectric constant of the metal, and Ω the solid angle directed to the angle θ.

The formation length of the forward radiation in vacuum is given by

$$Z_f=\frac{\beta\lambda}{2\pi(1-\beta\cos\theta)}\ . \tag{3}$$

In the far-infrared region, the formation length for a relativistic electron is considerably long. When the energy of the electron is 150 MeV, for example, the formation length is 13.8 m at the wavelength of $\lambda=1$ mm for the direction of $\theta=1/\gamma$, where γ is the Lorentz factor, $\gamma=1/(1-\beta^2)^{1/2}$. In the limited space of the laboratory, it is sometimes difficult to make the observation point far enough from the boundary to complete the emission process.

When a mirror to observe the forward TR is located within the formation length on the trajectory of the electron (see Fig. 1), the TR is partially suppressed [2]. Backward TR is also emitted from the mirror surface [13] and the observed TR will be the superposition of the forward TR from the foil and the backward TR from the mirror. The intensity and the angular distribution of TR should depend on an emission length, or the length between the foil and the mirror. However, there have been only a few investigations on the dependence of TR on the emission length. The effect of the emission length on the TR intensity was studied qualitatively in the x-ray region [14,15] using multifoil radiators with variable spacings

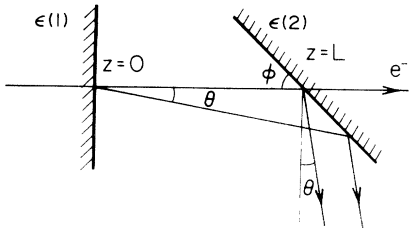

FIG. 1. Schematic diagram of a system of transition radiation. Electrons travel with a constant velocity along the z axis. A metallic foil and a mirror, whose dielectric constants are $\epsilon(1)$ and $\epsilon(2)$, are located on the trajectory. The trajectory is normal to the foil and has an incident angle of 45° to the surface of the mirror.

between the foils. Recently, Shibata *et al.* [5] observed the relation between the emission length and the intensity of the coherent TR in millimeter wavelengths, using electrons of 42 MeV from an L-band linear accelerator at Kyoto University. In the previous experiment [5], however, the bunch length was not short enough and the beam was not narrow enough to observe the coherent radiation in a complete enhancement. In the present experiment, we have used a very short bunch and a thin beam from an S-band LINAC at Tohoku University and have carried out more detailed observations.

In this paper we report properties of coherent TR in the far-infrared region emitted from the radiator composed of an upstream aluminum foil and a downstream mirror located within the formation length. (Hereafter, this radiator is referred to as an "aluminum-foil-mirror system.") In Sec. II we formulate the intensity of the TR from the radiator system, explicitly taking into account the emission length and the coherence effect. In Sec. III the experimental system is described, and in Sec. IV the experimental results are given and are compared with theory. We have observed the spectrum, the angular distribution of intensity, and the dependences of the intensity on the emission length and on the beam current. In Sec. V the bunch shape, or the distribution of the electrons in the bunch, has been derived from the spectrum. In Sec.VI the observed dependence of the TR intensity on the transverse spread of the electron beam is shown, and the result is discussed on the basis of the theory. In Sec. VII additional observations to clarify the property of TR are reported. The TR radiator is replaced by an Eccosorb sheet and the observed results are compared with those of the aluminum-foil-mirror system.

II. THEORY OF COHERENT TRANSITION RADIATION IN THE FAR-INFRARED REGION

A. Transition radiation emitted from an electron

We consider an electron passing through a metallic foil-mirror system which is shown in Fig. 1. The mirror is located downstream of the foil within the formation length to reflect the TR to the observer, and it also has the role of a TR radiator. The observed radiation is a superposition of TR from the foil and the surface of the mirror. The trajectory of the electron is normal to the foil, and an incident angle ϕ between the trajectory and the surface of the mirror is 45°. The dielectric constants of the foil and the mirror are $\epsilon(1)$ and $\epsilon(2)$.

Let the electron go along the z axis with a constant speed of v, the origin of the z axis be the emerging point of the electron in vacuum from the foil, and the electron cross the mirror surface at $z=L$. We call the distance between the foil and the mirror the emission length. In the case of the field downstream of the foil along the beam, the crossing term of electric vectors of the radiation and the charge field of the electron cannot be ignored [3], since the emission length L is smaller than the formation length Z_f in the present case. TR is emitted from both boundaries in a sequential process. In our experiment, however, TR is observed in a plane perpendicular to the beam axis. Hence, the phase difference between the charge field and the radiation fields is given by [3]

$$\Delta\psi=\frac{2\pi}{\beta\lambda}[L(1-\beta\cos\theta)-D\beta\cos\theta] , \tag{4}$$

where D is the distance of the observation point from the beam axis.

In the experiment, $D\gg\lambda$, so the phase difference is much larger than 2π and the radiation field is considered to be separated from the charge field. In other words, the interference term between the two fields oscillates rapidly, and its average over the space is negligible. We consider only the radiation field emitted from the two boundaries.

The intensity of TR is calculated using a method given by Pafomov and Frank [16]. The method is based on the theory that the Fourier component of the field in the frequency domain is equivalent to the field of a set of stationary dipoles located along the trajectory of the electron which have the moment $(ie/2\omega)\exp(i\omega z/v)$ per unit length [1].

We assume that the observation is made at a distant point much farther away than L and that the foil and the mirror are optically thick enough. Then, the TR intensity in units of photon number per unit solid angle per unit wavelength interval is given by

$$P=\frac{\alpha}{4\pi^2\lambda}\beta^2\sin^2\theta|P_c|^2 d\Omega\, d\lambda , \tag{5}$$

$$P_c=\frac{r_2 f_1}{\epsilon(1)^{1/2}\{1-\beta[\epsilon(1)-\sin^2\theta]^{1/2}\}}+\frac{r_2\{\exp[i\omega L(1-\beta\cos)/v]-1\}}{1-\beta\cos\theta}$$
$$+\frac{r_1 r_2\{\exp[i\omega L(1+\beta\cos\theta)/v]-1\}}{1+\beta\cos\theta}+\frac{\{\exp[i\omega L(1-\beta\sin\theta)/v]-1\}}{1-\beta\sin\theta}-\frac{f_2\exp[i\omega L(1-\beta\cos\theta)/v]}{\epsilon(2)^{1/2}[1+\beta\epsilon(2)^{1/2}\cos\theta_2]} , \tag{6}$$

where f_1 and r_1 are Fresnel coefficients of refraction and reflection of the foil and f_2 and r_2 are those of the mirror. Angle θ_2 is related to θ by the law of refraction:

$$\cos(\phi-\theta)=-\epsilon(2)^{1/2}\cos(\phi+\theta_2) .$$

The first term of Eq. (6) is a contribution from the integration of the field of the dipoles along the trajectory at upstream of the foil. The second to the fourth terms are those from the trajectory between the two boundaries: The second term corresponds to the radiation from the limited trajectory which propagates to the direction of the motion of the electron, the third term corresponds to the radiation which propagates backward and is reflected by the upstream foil, and the fourth term, which arises from the condition that the optical axis of the observation is perpendicular to the beam trajectory, represents radiation directly propagating to the observer. The last term of Eq. (6) is a contribution from the trajectory at downstream of the mirror surface.

The second term in Eq. (6) is most important for high-energy electrons, because the denominators is much less than unity for small values of angle θ. The first term is also important, since it may be comparable to the second term at proper values of θ, depending on the value of the dielectric constant of the upstream radiator. The other terms are smaller than the second term by at least one order of magnitude under the present experimental conditions. Ignoring these terms, we reduce Eq. (6) to

$$P_c=\frac{2}{(1-\beta\cos\theta)^2}R_2|\zeta'|^2[1-\cos(L/Z_f)] , \tag{7}$$

$$\zeta'=\frac{[1-\epsilon(1)\cos\theta][\epsilon(1)-\sin^2\theta]^{1/2}}{\{\epsilon(1)\cos\theta+[\epsilon(1)-\sin^2\theta]^{1/2}\}\{1-\beta[\epsilon(1)-\sin^2\theta]^{1/2}\}} , \tag{8}$$

$$R_2=\left|\frac{\epsilon(2)\sin(\phi-\theta)-[\epsilon(2)-\cos^2(\phi-\theta)]^{1/2}}{\epsilon(2)\sin(\phi-\theta)+[\epsilon(2)-\cos^2(\phi-\theta)]^{1/2}}\right|^2 , \tag{9}$$

where R_2 is the reflectivity of the mirror and is close to unity in the far-infrared region.

In our experiment, the following conditions are satisfied: $1-\beta\ll 1$, $|\epsilon(1)|>1$, and $\theta^2\ll 1$. So, the factor ζ' is almost equivalent to the ζ of Eq. (2), and its value is nearly equal to unity. Equation (5) is reduced to

$$P=2P_eR_2[1-\cos(L/Z_f)] , \tag{10}$$

where Z_f is the formation length and P_e is given by Eq. (1) with the replacement $\epsilon=\epsilon(1)$. When the ratio L/Z_f is much smaller than unity, the intensity is proportional to $(L/\lambda)^2$.

It is interesting to note that Eq. (10) is equal to a formula of interference given by Wartski *et al.* [13]. These authors have calculated the intensity as the result of interference between forward TR from an upstream foil and backward TR from a downstream foil separated by the distance L which is longer than Z_f. As shown above, Eq. (10) is proved to be applicable for any value of L.

Equation (10) is also equivalent to the formula for TR from a vacuum slab of thickness L in a dielectric medium, on the condition that $R_2=1$ [17].

B. Coherent radiation from bunched electrons

The TR expressed by Eq. (10) is emitted in a cone and its electric vector is in the plane given by the beam trajectory and the direction of observation [1–3]. When a bunch of electrons emit TR, the electric field at the observation point is given by superposition of the plane waves emitted from every electron:

$$\mathbf{E}=E_0\sum_{j=1}^{N}\frac{\mathbf{r}_j\times(\mathbf{V}_j\times\mathbf{r}_j)}{|\mathbf{r}_j\times(\mathbf{V}_j\times\mathbf{r}_j)|}\exp[i2\pi|\mathbf{r}_j|/\lambda] , \tag{11}$$

where vector $\mathbf{r}_j$ is a position vector from the jth electron to the observation point, $\mathbf{V}_j$ is the velocity of the electron, and N is the number of electrons in a bunch. The quantity $|E_0|^2$ is proportional to the TR intensity emitted from an electron.

When the cross section of the beam is small and the observation point is far from the emitting point, the intensity of TR is expressed by the analogy of the intensity of coherent synchrotron radiation [8,18,19] as

$$P_{\mathrm{TR}}(\lambda)=N[1+Nf(\lambda)]P(\lambda) , \tag{12}$$

where $P(\lambda)$ is the TR intensity emitted from an electron. The first term of Eq. (12) expresses the ordinary TR and the second term the coherent TR. The quantity $f(\lambda)$ is the bunch form factor which is given by the Fourier transform of the distribution function, $S(\mathbf{x})$, of an electron in the bunch:

$$f(\lambda)=\left|\int S(\mathbf{x})\exp[i2\pi(\mathbf{n}\cdot\mathbf{x})/\lambda]d\mathbf{x}\right|^2 , \tag{13}$$

where $\mathbf{n}$ is a unit vector directed from the center of the bunch to the observation point and $\mathbf{x}$ is a position vector of an electron relative to the bunch center. When we observe the TR from the on-axis or nearly on-axis direction, i.e., $\theta^2\ll 1$, the bunch form factor is given by

$$f(\lambda)=\left|\int S(\mathbf{z})\exp[i2\pi z/\lambda]dz\right|^2 , \tag{14}$$

where $S(z)$ is a one-dimensional distribution function of an electron projected onto the trajectory of the beam.

The value of $f(\lambda)$ varies from 0 (the incoherent limit) to 1 (the coherent limit). The intensity of the coherent TR is proportional to the square of N, and in the coherent limit it is enhanced by a factor of N in comparison with that of incoherent TR.

When the transverse size of the electron beam is considerably larger than the wavelength of the radiation, the value of $f(\lambda)$ decreases [19]. This effect is discussed in Sec. VI.

III. EXPERIMENT

The experimental arrangements for generating TR are shown in Figs. 2(a) and 2(b). Electrons were accelerated to 150 MeV by the Tohoku 300-MeV LINAC with the rf frequency of 2856 MHz. The duration of a burst of electrons was 2 μs, and its repetition rate was 300 pulses/s.

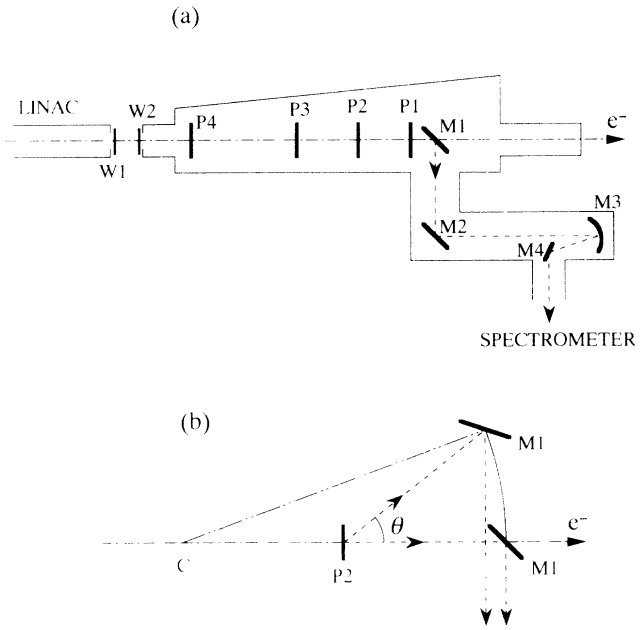

FIG. 2. Schematic diagram of the experiment: (a) A dot-dashed line shows the trajectory of the electron beam. M1, M2, and M4 are plane mirrors and M3 is a spherical mirror. W1 and W2 are titanium windows. The position of an upstream foil is varied from points P1 to P4. (b) Assembly to observe the angular distribution of transition radiation. The mirror M1 is rotated around a vertical axis C.

The energy spread of the electrons was 0.2%, and the average beam current was typically 1 μA, which corresponds to 3.6×10^6 electrons in a bunch.

The vacuum chamber to generate TR was separated from the linac by 50-μm-thick titanium windows W1 and W2, as shown in Fig. 2(a). The distance between the two windows was 50 mm. The residual gas pressure in the chamber was less than 1 Pa, which was far below the Cherenkov threshold in air, 2.17×10^3 Pa.

On the beam trajectory, we placed a radiator system composed of an aluminum foil of size (width$\times$height$\times$thickness) $50\times100\times0.015$ mm^3 and a plane mirror M1, which was an aluminum-evaporated fused silica, of size $75\times50\times1$ mm^3.

To observe dependence of the TR intensity on the emission length, i.e., the distance between the foil and the mirror M1, the aluminum foil was moved from point P1 to point P4 in Fig. 2(a). The emission lengths were 41, 156, 350, and 872 mm at the points P1, P2, P3, and P4, respectively. In the case of the observation of the angular distribution of the TR, the mirror M1 was rotated around an axis C as shown in Fig. 2(b). The transverse beam size (width$\times$height) of the electrons was 5×7 mm^2 at point P2.

The TR was collected by a spherical mirror M3 with an acceptance angle of 70 mrad and was led to a grating-type far-infrared spectrometer [9], which was equipped with a monitor system to correct the fluctuation of the intensity due to the beam instability. The radiation was detected by a liquid-helium-cooled Si bolometer. The spectral sensitivity of the measuring system was calibrated by a source of blackbody radiation at 1200 K [9]. The observational error of the measuring system in the absolute intensity was estimated to be within a factor of 1.5.

IV. RESULTS AND DISCUSSION

A. Spectrum

Spectral intensities of TR from the aluminum-foil-mirror system were observed in the wavelength range from 0.2 to 5 mm. The results from the emission lengths L of 156 (A) and 872 (B) mm are shown in Fig. 3. A spectrum for $L=350$ mm was also measured, which lay between the two spectra for $L=156$ and 872 mm, though it is not shown in Fig. 3. The intensity increased with the emission length in the whole observed wavelength region. All spectra had similar structures with a broad peak at about $\lambda=1$ mm and the intensity decreased sharply towards shorter wavelengths.

Theoretical intensities of the incoherent TR are calculated by Eq. (10) on the experimental conditions and are shown by dashed curves in Fig. 3. The observed intensity at $\lambda=1$ mm with $L=156$ mm is enhanced by a factor of 0.9×10^6 compared with the calculated intensity of the incoherent TR. The factor of the enhancement is of the same order of magnitude as the number of electrons in the bunch, 3.6×10^6.

B. Dependence of intensity on the emission length

The TR intensity was observed by changing the emission length L from 41 to 872 mm at wavelengths of $\lambda=0.7$, 1.4, 2.4, and 4.5 mm. The observed intensities at each wavelength have been normalized to the intensity at $L=156$ mm and the results are shown in Fig. 4 by open circles. The intensity increases with the emission length

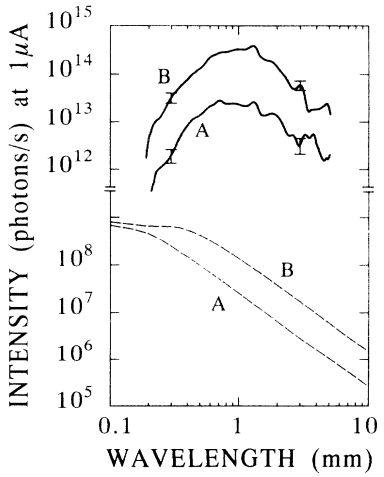

FIG. 3. Observed spectra of the transition radiation of an aluminum-foil-mirror system from the emission lengths of 156 (A) and of 872 (B) mm. The intensity is given in units of photons per second per 1% bandwidth ($\Delta\lambda/\lambda=0.01$) at the beam current of 1 μA. Vertical bars show observational errors. The dashed lines show theoretical intensities of incoherent transition radiation from $L=156$ (A) and 872 (B) mm.

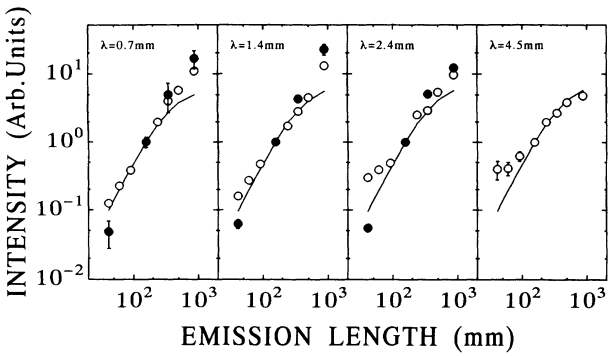

FIG. 4. Dependence of the intensity of the transition radiation on the emission length. The open circles show radiation from the aluminum-foil-mirror system and the solid circles that from the Eccosorb-mirror system. Theoretical intensities are shown by the solid curves.

at all wavelengths.

The solid curves show the theoretical intensity of the incoherent TR. The observed points at each wavelength are in good agreement with the calculation. At short wavelengths, however, the observed intensity from the long emission length is more intense than the calculation. At $\lambda=4.5$ mm, on the other hand, the observed intensities from the emission length of less than 100 mm were larger than the calculation. According to a further experiment we have performed, these deviations are related to the transverse spread of the electron beam. Detailed experiments and analysis of the results will be reported in a separate paper.

C. Dependence of intensity on the beam current

The TR intensity from the emission length of 872 mm was measured by controlling the beam current by a profile-defining slit of the LINAC and thus varying the number of electrons in a bunch. The results are shown in Fig. 5; the open circles, solid circles, and squares show the intensities at the wavelengths of $\lambda=0.7$, 1.4, and 2.4 mm, respectively.

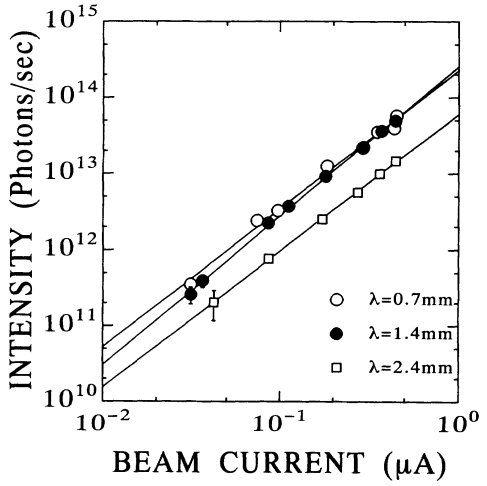

FIG. 5. Dependence of the intensity of transition radiation on the beam current. The straight lines are fitted to the data by the method of least squares and the gradients are 1.82 ± 0.04, 1.96 ± 0.02, and 1.86 ± 0.01 for $\lambda=0.7$, 1.4, and 2.4 mm, respectively.

The straight lines in Fig. 5 have been determined by method of least squares. Their gradients are 1.82 ± 0.04, 1.96 ± 0.02, and 1.86 ± 0.01 at $\lambda=0.7$, 1,4, and 2.4 mm, respectively, and are close to 2. This result shows that the intensity is nearly proportional to the square of the number of electrons in a bunch and that coherent TR has been observed.

D. Angular distribution

The angular distribution of TR intensity was observed and the results for the emission length of 350 mm at the wavelengths of 1.4 and 2.4 mm are shown in Fig. 6(a). In the Figure the distribution of the total intensity is shown by the solid curves, and the horizontal and vertical components are shown by the dashed and dotted curves, respectively.

The observed distributions are almost symmetric with respect to the angle $\theta=0$, i.e., with respect to the direction of the electron beam. The distribution of the total intensity has two main peaks at angle θ around ±100 mrad. The angle between the two peaks corresponds to the apex angle of the light cone of the TR. The dependence of the angle on the wavelength for three emission lengths $L=156$, 350, and 872 mm is shown in Fig. 7 by open circles, solid circles, and squares, respectively. The TR diverges more as the wavelength increases and as the emission length decreases.

For comparison, the theoretical angular distribution of the incoherent TR intensity collected by the optical system with an acceptance angle of 70 mrad has been calculated on the basis of Eq. (10). In the calculation the size of the mirror M1 has been assumed to be unbounded. The results for $L=350$ mm at $\lambda=1.4$ and 2.4 mm are shown in Fig. 6(b). The distributions of the horizontal component, the vertical one, and the total intensity are shown by the dashed, dotted, and solid curves, respec-

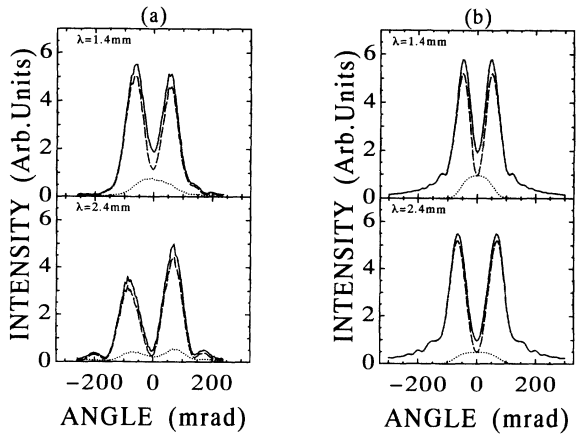

FIG. 6. The angular distribution of the intensity of the transition radiation from the emission length of 350 mm obtained by (a) the observation and (b) the theoretical calculation. The solid, dashed, and dotted curves show the total intensity and the horizontally and vertically polarized components of the radiation, respectively.

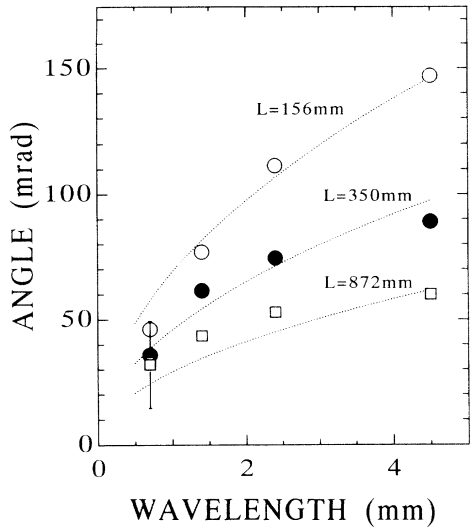

FIG. 7. Dependence of the main peak angle on the wavelength for three emission lengths: $L=156$, 350, and 872 mm. The dotted curves show the theoretical relation given by Eq. (18) in the text.

tively. The calculated distribution is in fairly good agreement with the observation.

According to theory [2,12], when $L \gg Z_f$, most of the TR is emitted in the direction of $\theta=1/\gamma$. In the present experiment, however, the emission length is much shorter than the formation length, i.e., $L \ll Z_f$. In addition, the value of $1-\beta$ is 5.8×10^{-6}, which is much less than unity, and we have made the observation in the direction of small angle $\theta^2 \ll 1$. Then, the TR intensity of Eq. (10) is given as follows [5]:

$$P=\alpha\left[\frac{L}{\lambda}\right]^2\left[\frac{d\lambda}{\lambda}\right]|\zeta|^2\sin^2\theta\left[\frac{\sin X}{X}\right]^2 d\Omega\ , \tag{15}$$

$$X=\frac{\pi L}{2\lambda}\left[\frac{1}{\gamma^2}+\theta^2\right]\ . \tag{16}$$

The angular dependence of the intensity expressed by Eq. (15) has the following properties: The angular distribution of the TR has an oscillatory structure, and the maximum flux of the TR is emitted in the direction of the first peak whose angle θ_p is determined from the equation

$$\frac{\tan X}{X}=\frac{2\theta_p^2}{\theta_p^2-1/\gamma^2}\ . \tag{17}$$

When $\theta_p^2 \gg 1/\gamma^2$, θ_p is given approximately by

$$\theta_p \sim 0.86(\lambda/L)^{1/2}\ . \tag{18}$$

The condition $\theta_p^2 \gg 1/\gamma^2$ is equivalent to $\lambda/L \gg 1/\gamma^2$, i.e., the emission length L is much shorter than the formation length along the beam axis. When λ/L decreases, θ_p approaches $1/\gamma$. The approach, however, is not smooth, since the maximum TR flux shifts from the first peak to the second and so on as λ/L decreases. The value of the peak angle given by Eq. (18) is valid for the range $\lambda/L > 2\pi/\gamma^2$ within an accuracy of 6%. It is interesting to note that these properties of TR in the long-wavelength region are the same as those of Cherenkov radiation from a limited length of a trajectory [5,20].

The relation between the peak angle and the emission length given by Eq. (18) is shown by dotted curves in Fig. 7. The observed peak angles for three emission lengths are in good agreement with theory.

Besides the main peaks, the observed angular distributions in Fig. 6(a) have small subsidiary peaks at larger angles. In the observation of the angular distribution of the TR, the mirror M1 has a limited size and it gets out of the beam for angles $|\theta| > 160$ mrad [see Fig. 2(b)]. At the direction of $\theta=160$ mrad, the formation length at $\lambda=5$ mm is 62.5 mm and is smaller than the emission length of 156 mm. At angles smaller than but near to 160 mrad, interference should occur between the forward TR from the foil and the backward TR from the mirror. For the angles $|\theta| > 160$ mrad, on the other hand, Eq. (10) should be replaced by $P=R_2P_e$, which is only the forward TR from the aluminum foil reflected by the mirror, and the angular distribution should not show oscillatory structure due to the interference effect. The observed angular distributions of TR in Fig. 6(a) at large angles, however, show complex oscillatory structure: At the wavelength $\lambda=2.4$ mm, the secondary peak is seen at the angle around ±180 mrad. The distribution at $\lambda=1.4$ mm also shows the secondary peak as a shoulder at the angle around ±150 mrad and the third peak around ±200 mrad. It is not clear at present what caused the oscillatory structure.

V. BUNCH FORM FACTOR AND ELECTRON DISTRIBUTION IN A BUNCH

A bunch form factor has been derived from the observed spectrum of coherent TR and the theoretical intensity of incoherent TR. Figure 8 shows the form factor derived from the spectrum of the emission length of 156 mm.

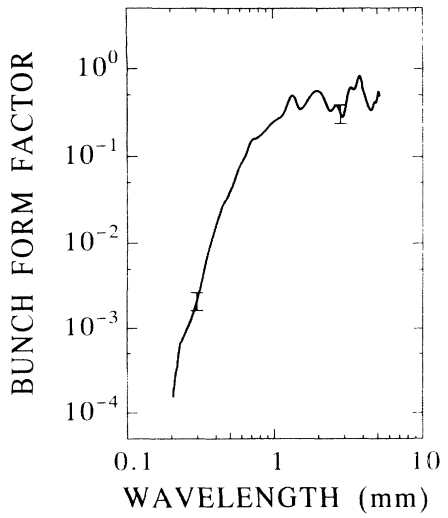

FIG. 8. Bunch form factor derived from the observed spectrum of the transition radiation from the aluminum-foil-mirror system.

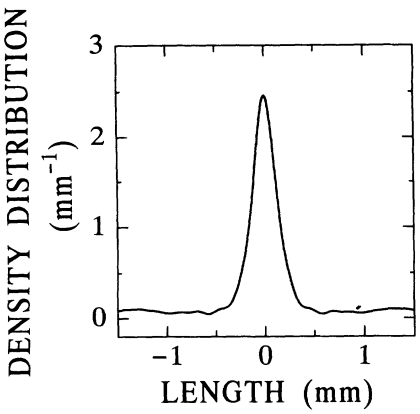

FIG. 9. Distribution of electrons in a bunch derived from the bunch form factor in Fig. 8. The bunch length along the longitudinal direction (FWHM) is 0.28 mm.

The electron distribution in a bunch has been obtained from Eq. (14) by the inverse Fourier transform of the form factor. The result is shown in Fig. 9. The distribution resembles a Gaussian function in shape, and the bunch length [full width at half maximum (FWHM)] is 0.28 mm. The distribution of electrons in a bunch is almost the same as that derived previously from the spectrum of coherent synchrotron radiation, using the same LINAC [9]. The bunch length obtained from the spectrum is shorter than 1.7 mm, which was estimated from the accelerating mechanism of the LINAC [7]. Possible reasons for the difference were discussed previously [9].

The transverse spread of the electron beam diminishes the form factor. In the present experiment, however, the effect is negligible in the long-wavelength region where the form factor in Fig. 8 has large values, as is discussed in Sec. VI.

According to the definition of the distribution function of electrons in the bunch, the integration of $S(z)$ should be equal to unity. From the distribution of electrons derived from the observation, which is shown in Fig. 9, we have evaluated the integration. The result is $\int S(z)dz = 0.7$. If we consider the accuracy of the factor of 1.5 in the measurement of the absolute intensity of the spectrum, this value is in agreement with unity.

VI. EFFECT OF BEAM SIZE ON TRANSITION RADIATION

To observe the dependence of coherent TR on the transverse size of the electron beam, the cross section of the beam at the emitting point was varied by a pair of quadrupole magnets located at about 10 m upstream from the TR radiator. The cross section was elliptic and the size (horizontal×vertical) changed from (a) 5×7 mm^2 to (b) 14×12 mm^2 and to (c) 24×21 mm^2. The angular distribution of the TR was measured at three wavelengths $\lambda=1.4$, 2.4, and 4.5 mm for the emission length $L=156$ mm. The results are shown in Fig. 10, where the curves *a*, *b*, and *c* correspond to the three beam sizes. As the beam size increased, the intensity decreased greatly and the divergence of TR also decreased.

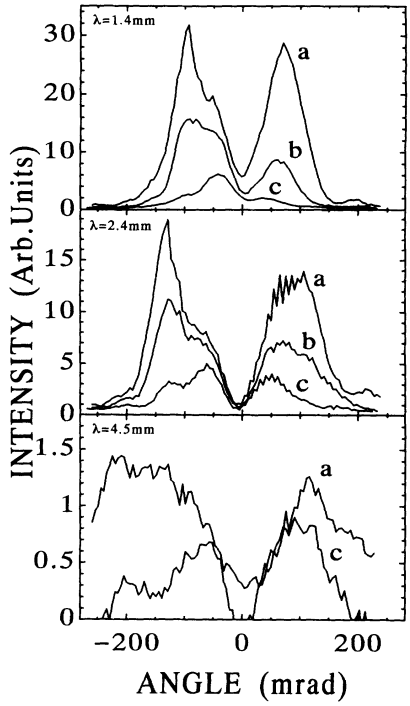

FIG. 10. Angular distribution of transition radiation from spread electron beams at $\lambda=1.4$, 2.4, and 4.5 mm. The transverse beam sizes are (a) 5×7 mm^2, (b) 14×12 mm^2, and (c) 24×26 mm^2.

These results are explained by an interference effect of TR which is emitted from different positions in the cross section of the beam. As the longitudinal bunch length obtained in Sec. V is 0.28 mm, we assume for simplicity that electrons are uniformly distributed in a disk whose thickness is negligibly small in comparison with the wavelength and that the direction of motion of each electron is parallel to the z axis. Assuming that the observation point is far from the emitting point, the form factor in Eq. (13) is calculated as follows:

$$f(\lambda)=\left\{\frac{J_1[2\pi(\rho/\lambda)\sin\theta]}{\pi(\rho/\lambda)\sin\theta}\right\}^2, \tag{19}$$

where J_1 is the Bessel function of the order 1 and ρ is the radius of the disk. Equation (19) shows that $f(\lambda)=1$ for $\rho/\lambda \ll 1$ and that as $(\rho/\lambda)\sin\theta$ increases, $f(\lambda)$ decreases first and begins to oscillate with gradually decreasing amplitude. The effect of the transverse beam spread becomes prominent with the increase of the argument $(\rho/\lambda)\sin\theta$.

Using the bunch form factor of Eq. (19), we have calculated the angular distribution of coherent TR for the emission length $L=156$ mm. The results at $\lambda=1.4$, 2.4, and 4.5 mm are shown in Fig. 11 for three beam diameters: of (a) 6, (b) 13, and (c) 25 mm. The figure shows that the divergence and the intensity of TR decreases with the beam diameter and that the main peaks finally converge into one central peak at the beam of larger diameter. This is qualitatively in good agreement with the observation.

To examine the effect of the transverse spread of beams

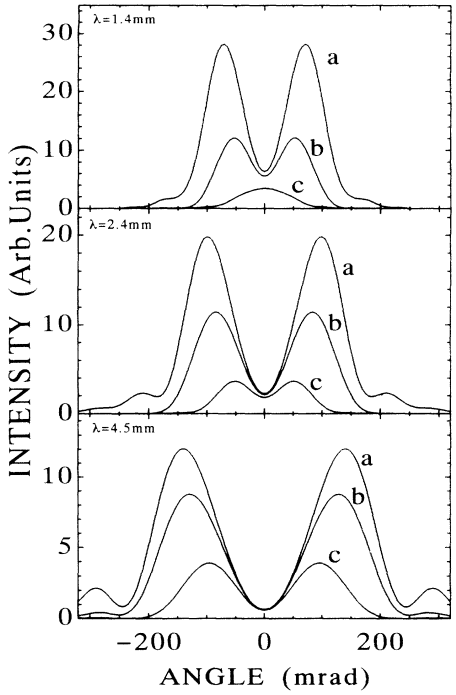

FIG. 11. Theoretical angular distribution of the transition radiation at $\lambda=1.4$, 2.4, and 4.5 mm calculated on the assumptions that electrons are distributed uniformly in a thin disk and that the disk plane is normal to the trajectory. Curves *a*, *b*, and *c* correspond to the disk diameters of 6, 13, and 25 mm, respectively.

on the spectral intensity shown in Fig. 3, numerical calculation has been carried out on the basis of Eq. (19) and the experimental conditions. A ratio of the TR intensity with the beam spread to that without the spread has been calculated. The ratio is larger than 0.95 in the wavelength region $\lambda > 1.2$ mm and decreases as the wavelength decreases. It is 0.82 at $\lambda=0.6$ mm and is 0.64 at $\lambda=0.4$ mm. These results confirm that the form factor in Fig. 8 is reliable in the long-wavelength region $\lambda > 0.6$ mm with an accuracy of better than 20%.

VII. TRANSITION RADIATION FROM ECCOSORB SHEET

The intensity of TR depends on the properties of two radiators in Fig. 2. To examine the dependence, the composition of the radiators was changed as follows: First, we replace the aluminum foil by a sheet of Eccosorb AN72 (Emerson & Cuming Co.) with a thickness of 6 mm, an absorber of millimeter waves. TR from the Eccosorb-mirror system is compared with that of the aluminum-foil-mirror system. Next, the mirror was also replaced by the Eccosorb sheet, and TR from the Eccosorb-Eccosorb system was measured.

The dielectrc constant of the Eccosorb sheet was estimated from a technical sheet of the manufacturer as $\epsilon=1.3+0.5i$ at $\lambda=3$ mm, and both real and imaginary parts of the constant increased with the wavelength. So the factor ζ' of Eq. (8) is well approximated by unity in the wavelength region considered here. The Eccosorb sheet as the forward radiator should have the same role

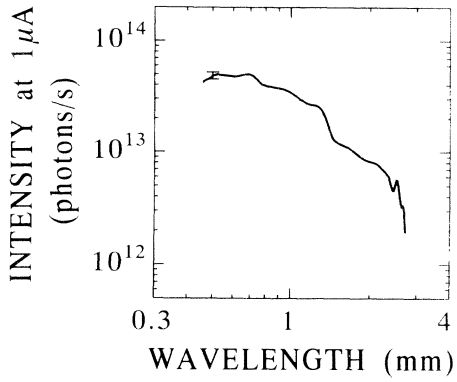

FIG. 12. Observed spectra of the transition radiation of the Eccosorb-mirror system from the emission length of 156 mm.

as the aluminum foil [5]. On the other hand, reflectvity of the Eccosorb sheet is 1% at $\lambda=15$ mm (frequency, 20 GHz) and decreases toward shorter wavelengths. According to Eq. (10), the replacement of the mirror by the Eccosorb sheet should cause a drastic change in the TR intensity.

A. Transition radation from the Eccosorb-mirror system

The sheet of Eccosorb was used in the place of a metallic foil in Fig. 2. The TR intensity from the Eccosorb-mirror system for $L=156$ mm was observed in the wavelength range from 0.45 to 3 mm and is shown in Fig. 12. The observed intensity at $\lambda=1$ mm is enhanced by a factor of 1.3×10^6 in comparison with the theoretical intensity of incoherent TR. As expected, the spectral intensity of the Eccosorb-mirror system in the wavelegth range $\lambda > 1$ mm is the same as that of the aluminum-foil-mirror system in Fig. 3 within the accuracy of the observation. The spectrum, however, shows a small discrepancy: The

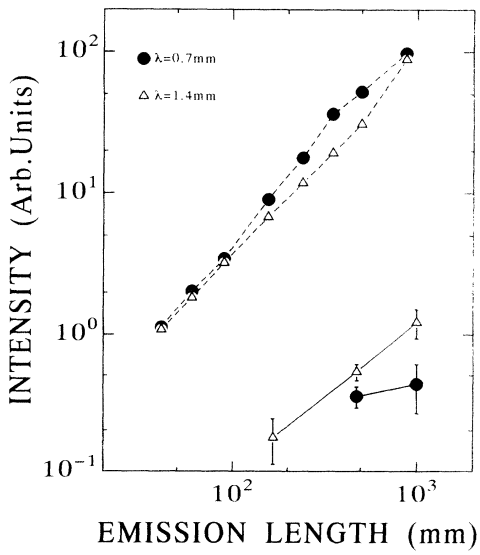

FIG. 13. The intensity of the transition radiation from the Eccosorb-Eccosorb system (solid lines) at $\lambda=0.7$ (circles) and 1.4 mm (triangles). For comparison, the observed intensity of the Eccosorb-mirror system is also shown by dashed lines.

spectral intensity of the Eccosorb-mirror system in the short-wavelength range was stronger than that of the aluminum-foil-mirror system. The reason for the difference is not clear at present, but it is possible that some of the beam conditions have changed slightly.

The TR intensity from the Eccosorb-mirror system was observed by changing the emission length L from 41 to 872 mm at $\lambda=0.7$, 1.4, and 2.4 mm. The relative intensities normalized to the intensity at $L=156$ mm are plotted in Fig. 4 by the solid circles. The observed relation is roughly in agreement with theory, although the slope of the intensity–emission length relation of the Eccosorb-mirror system in Fig. 4 is a little steeper than the theoretical one.

B. Transition radiation from the Eccosorb-Eccosorb system

The TR intensity from the Eccosorb-Eccosorb system was measured, and the results at $\lambda=0.7$ and 1.4 mm are shown in Fig. 13 by solid lines. The dashed lines in the figure shows the TR intensity of the Eccosorb-mirror system for comparison. The observed intensities of the Eccosorb-Eccosorb system were weaker by about two orders of magnitude than that of the Eccosorb-mirror system. As the reflectivity of the Eccosorb sheet R_2 is lower than 1%, the result is in accord with the theoretical expectation.

ACKNOWLEDGMENTS

We thank the machine group of the Laboratory of Nuclear Science, Tohoku University, and Mr. T. Tsutaya of the Research Institute for Scientific Measurements for their technical support. We also thank Professor K. Niizeki, Professor S. Takagi, and Professor Y. Kayanuma of the Department of Physics for elucidating discussions. This work was partially supported by a Grant-in-Aid for Scientific Research from the Ministry of Education, Science, and Culture of Japan.

[1] V. L. Ginzburg and I. M. Frank, Zh. Eksp. Teor. Fiz. **16**, 15 (1946).
[2] F. G. Bass and V. M. Yakovenko, Usp. Fiz. Nauk **86**, 189 (1965) [Sov. Phys. Usp. **8**, 420 (1965)].
[3] V. L. Ginzburg and V. N. Tsytovich, *Transition Radiation and Transition Scattering* (Adam Hilger, Bristol, 1990).
[4] Y. Shibata, K. Ishi, T. Takahashi, F. Arai, M. Ikezawa, K. Takami, T. Matsuyama, K. Kobayashi, and Y. Fujita, Phys. Rev. A **44**, R3449 (1991).
[5] Y. Shibata, K. Ishi, T. Takahashi, T. Kanai, M. Ikezawa, K. Takami, T. Matsuyama, K. Kobayashi, and Y. Fujita, Phys. Rev. A **45**, R8340 (1992).
[6] U. Happek, A. J. Sievers, and E. B. Blum, Phys. Rev. Lett. **67**, 2962 (1991).
[7] T. Nakazato, M. Oyamada, N. Niimura, S. Urasawa, O. Konno, A. Kagaya, R. Kato, T. Kamiyama, Y. Torizuka, T. Nanba, Y. Kondo, Y. Shibata, K. Ishi, T. Ohsaka, and M. Ikezawa, Phys. Rev. Lett. **63**, 1245 (1989).
[8] Y. Shibata, K. Ishi, T. Ohsaka, H. Mishiro, T. Takahashi, M. Ikezawa, Y. Kondo, T. Nakazato, M. Oyamada, N. Niimura, S. Urasawa, R. Kato, and Y. Torizuka, Nucl. Instrum. Methods Phys. Res. A **301**, 161 (1991).
[9] K. Ishi, Y. Shibata, T. Takahashi, H. Mishiro, T. Ohsaka, M. Ikezawa, Y. Kondo, T. Nakazato, S. Urasawa, N. Niimura, R. Kato, Y. Shibasaki, and M. Oyamada, Phys. Rev. A **43**, 5597 (1991).
[10] Y. Shibata, T. Takahashi, K. Ishi, F. Arai, H. Mishiro, T. Ohsaka, M. Ikezawa, Y. Kondo, S. Urasawa, T. Nakazato, R. Kato, S. Niwano, and M. Oyamada, Phys. Rev. A **44**, R3445 (1991).
[11] E. B. Blum, U. Happek, and A. J. Sievers, Nucl. Instrum. Methods Phys. Res. A **307**, 568 (1991).
[12] G. M. Garibian, Zh. Eksp. Teor. Fiz. **33**, 1403 (1957) [Sov. Phys. JETP **6**, 1079 (1958)]; **37**, 527 (1959) [**10**, 372 (1960)].
[13] L. Wartski, S. Roland, J. Lasalle, M. Bolore, and G. Filippi, J. Appl. Phys. **46**, 3644 (1975).
[14] L. C. L. Yuan, C. L. Wang, H. Uto, and S. Prünster, Phys. Rev. Lett. **25**, 1513 (1970).
[15] M. L. Cherry, G. Hartmann, D. Muller, and T. A. Prince, Phys. Rev. D **10**, 3594 (1974).
[16] V. E. Pafomov and I. M. Frank, Yad. Fiz. **5**, 631 (1967) [Sov. J. Nucl. Phys. **5**, 448 (1967)].
[17] L. Durand, Phys. Rev. D **11**, 89 (1975).
[18] J. S. Nodvick and D. S. Saxon, Phys. Rev. **96**, 180 (1954).
[19] L. A. Vardanyan, G. M. Garibyan, and C. Yang, Izb. AN. Armenian SSR Fiz. **10**, 350 (1975).
[20] J. R. Neighbours, F. R. Buskirk, and A. Saglam, Phys. Rev. A **28**, 1531 (1983).